

Numerical Synthesis of Six-bar Linkages for Mechanical Computation

M. Plecnik

Robotics and Automation Laboratory,
University of California, Irvine
mplecnik@uci.edu

J. M. McCarthy

Robotics and Automation Laboratory,
University of California, Irvine
jmmccart@uci.edu

ABSTRACT

This paper presents a design procedure for six-bar linkages that use eight accuracy points to approximate a specified input-output function. In the kinematic synthesis of linkages, this is known as the synthesis of a function generator to perform mechanical computation. Our formulation uses isotropic coordinates to define the loop equations of the Watt II, Stephenson II, and Stephenson III six-bar linkages. The result is 22 polynomial equations in 22 unknowns that are solved using the polynomial homotopy software Bertini. The bilinear structure of the system yields a polynomial degree of 705,432. Our first run of Bertini generated 92,736 nonsingular solutions, which were used as the basis of a parameter homotopy solution. The algorithm was tested on the design of the Watt II logarithmic function generator patented by Svoboda in 1944. Our algorithm yielded his linkage and 64 others, in 129 minutes of parallel computation on a Mac Pro with 12×2.93 GHz processors. Three additional examples are provided as well.

1 Introduction

This paper presents a methodology for the design of mechanical computers that approximate a function specified by eight angular pairs of accuracy points. This is known as the kinematic synthesis of a function generator, see Hartenberg and Denavit [1], Kinzel et al. [2], Plecnik and McCarthy [3] and Kim et al. [4]. In 1944, Svoboda [5] used a nomograph formulation to design a six-bar linkage that generates a logarithmic function, which he called a “double-three bar” because it is a Watt II type six-bar that can be viewed as two connected four-bar linkages. More recently Hwang and Chen [6] present a methodology for the synthesis of six-bar function generators of the Stephenson II type.

This work uses isotropic coordinates to formulate the loop equations of three types of six-bar linkages that are useful for function generation, the Watt II, Stephenson II and Stephenson III types, see Fig. 1. For each linkage type, we specify eight pairs of input-output joint angles, (ϕ_j, ψ_j) , $j = 1 \dots 8$, called accuracy points, that satisfy a specified input-output function. Two constraint equations and one normalization condition are obtained from each of eight accuracy points which leads to a system of 24 nonlinear equations in 24 unknowns. This system can be simplified to obtain 22 bilinear equations in 22 unknowns, which has a maximum of 705,432 solutions.

The polynomial homotopy continuation software Bertini was used to solve the synthesis equations to yield 92,736 nonsingular solutions in 107 minutes on a Mac Pro with 12×2.93 GHz processors. This solution was then used in a parameter homotopy to design linkages for three different examples of function specification.

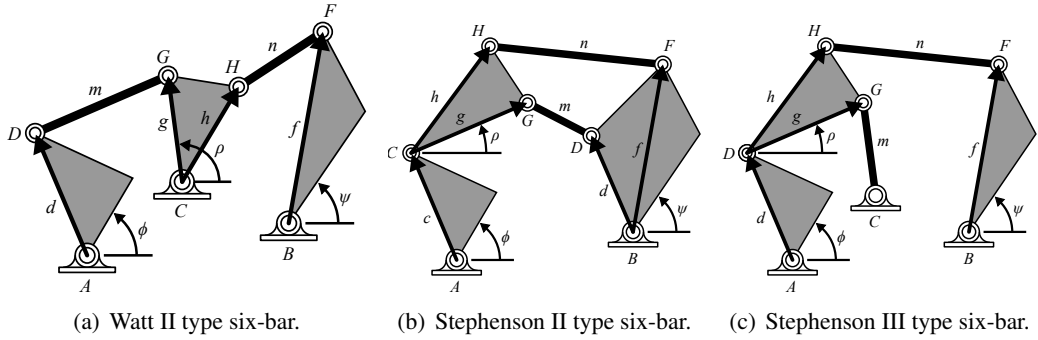


Fig. 1. The three types of Watt and Stephenson six-bar linkages that are useful for mechanical computation at fixed pivots. The angle ϕ at the fixed pivot A is the input value and the angle ψ at the fixed pivot B is the output value of the function.

2 Literature Review

A mechanical computer is linkage system that calculates an output for a given input, also called function generator. Svoboda [5] designed function generators by fitting the input-output functions of a given set of linkages to the desired function. He patented a Watt II type six-bar linkage that computed a logarithmic function [7]. Freudenstein 1954 [8] introduced a new approach that used the loop equations of a four-bar linkage to fit a given set of accuracy points to obtain a four-bar function generator.

McLarnan [9] formulated the loop equations for three types of six-bar linkages, the Watt II, Stephenson II and III types, to design function generators. He obtained algorithms for six, seven, eight and nine accuracy points for the Watt II six-bar linkage, which were executed on an IBM 704 computer. He obtained two Watt II linkages that achieved seven accuracy points, and noted the problem of the separation of accuracy points on different linkage branches, now known as a branch defect. Almost two decades later, Dhingra et al. 1994 [10] formulated the synthesis equations for Watt II, Stephenson II and III function generators and used a numerical homotopy algorithm to solve these equations. They report 1.5 seconds to track each of 71,680 homotopy paths for eight accuracy points on an 486 PC. This is approximately 30 hours to complete one synthesis calculation, and does not include the analysis of each design to verify that its accuracy points are on the same branch.

Recently, Hwang and Chen [6] formulated the design of Stephenson II six-bar function generators fusing optimization techniques to find defect-free linkages. Sancibrian [11] takes a similar approach using the Generalized Reduced Gradient to find the linkage parameters that minimize the difference between the input-output function of the linkage and the desired function.

In this paper, we formulate complex versions of the loop equations for the Watt II, Stephenson II and III six-bar linkages and use numerical homotopy to solve the equations, see Wampler et al. [12], Wampler [13] and Sommese and Wampler [14]. Our focus is fitting a function generator to eight accuracy points, which yields 22 synthesis equations in 22 unknowns. In order to find Watt II, and Stephenson II and III six-bar function generators that have the eight accuracy points on a single branch, we also analyze each of the resulting designs to verify its performance.

3 Complex Vectors and Isotropic Coordinates

Erdman et al. [15] formulate planar kinematics using complex numbers to represent the coordinates of points in the plane. In this formulation, the coordinates $P = (P_x, P_y)$ of a point are formulated as the complex number,

$$P = P_x + iP_y. \quad (1)$$

The component-wise sum of a complex number is the same as for coordinate vectors, and the product of complex numbers performs rotation and scaling operations. In particular, the exponential $\exp(i\theta)$ is a rotation

operator on complex vectors that yields the same result as a 2×2 rotation matrix operating on vectors, that is,

$$\begin{aligned} P &= \exp(i\theta)p, \\ P_x + iP_y &= (\cos\theta + i\sin\theta)(p_x + ip_y), \\ P_x - iP_y &= (\cos\theta p_x - \sin\theta p_y) + i(\sin\theta p_x + \cos\theta p_y). \end{aligned} \quad (2)$$

Wampler [13] shows that it is convenient to consider the complex number P and its conjugate \bar{P} as components of “isotropic coordinates”, (P, \bar{P}) , because the original components are obtained from the linear transformations,

$$P_x = \frac{1}{2}(P + \bar{P}), \quad P_y = \frac{1}{2i}(P - \bar{P}). \quad (3)$$

For our purposes, the reference to isotropic coordinates means that both the complex and complex conjugate loop equations are used in the formulation of the synthesis equations.

4 Synthesis Equations

The formulation of the synthesis equations for Watt II, Stephenson II and III function generators closely parallel each other. Note that synthesis of the Watt I and Stephenson I mechanisms was not studied because coordination between their ground pivots results in four-bar synthesis. Function generation involving moving pivots was not studied in this paper.

In this section, the loop equations are formulated for each topology, a normalization condition is appended for each accuracy point, then each system of equations is put into the polynomial form shown in Eqn. 35. Putting all three topologies into this form allows us to compute solutions to a single general polynomial system that can be used to construct straight-line homotopies for all three topologies that are computationally less expensive [16]. The solutions to these systems using the Bertini software are described in Section 5.

4.1 Watt II Synthesis Equations

The synthesis task for a Watt II function generator is to coordinate the orientation of links AD and BF such that they move through the angle pairs (ϕ_j, ψ_j) , $j = 1, \dots, 8$. Note that the input-output functions between link CGH and links AD or BF are not of interest because these are four-bar function generators.

Three sets of complex numbers are introduced to represent the rotations of links AD , CGH , and BF measured relative to the ground frame,

$$\begin{aligned} (Q_j, \bar{Q}_j) &= (\exp(i\phi_j), \exp(-i\phi_j)), \\ (R_j, \bar{R}_j) &= (\exp(ip_j), \exp(-ip_j)), \\ (S_j, \bar{S}_j) &= (\exp(i\psi_j), \exp(-i\psi_j)), \quad j = 1, \dots, 8. \end{aligned} \quad (4)$$

The complex vectors (Q_j, \bar{Q}_j) and (S_j, \bar{S}_j) are known from the task specification, while (R_j, \bar{R}_j) are to be determined in the synthesis process.

The loop equations of the Watt II linkage are formulated to define the two floating links DG and FH , as

$$\begin{aligned} \mathcal{L}_1 : \quad G - D &= A + dQ_j - C - gR_j, \\ \mathcal{L}_2 : \quad H - F &= B + fS_j - C - hR_j, \quad j = 1, \dots, 8. \end{aligned} \quad (5)$$

The constraints that the lengths $m = |G - D|$ and $n = |H - F|$ be constant for the movement of the six-bar linkage

yield the equations,

$$\begin{aligned}\mathcal{C}_1 : & (A + dQ_j - C - gR_j)(\bar{A} + \bar{d}\bar{Q}_j - \bar{C} - g\bar{R}_j) = m^2, \\ \mathcal{C}_2 : & (B + fS_j - C - hR_j)(\bar{B} + \bar{f}\bar{S}_j - \bar{C} - \bar{h}\bar{R}_j) = n^2,\end{aligned}\quad j = 1, \dots, 8. \quad (6)$$

Note that in the equations above $g = \bar{g}$ as the angle of ρ measures directly to this complex vector. The 16 constraint equations (6) together with the eight equations defining the pairs (R_j, \bar{R}_j) as unit vectors,

$$R_j \bar{R}_j = 1, \quad j = 1, \dots, 8, \quad (7)$$

yield 24 synthesis equations. The unknowns of these equations are the 16 values of (R_j, \bar{R}_j) and the eight unknowns, $(C, \bar{C}, d, \bar{d}, f, \bar{f}, m, n)$. The designer is free to specify the fixed pivots A and B and the dimensions g and (h, \bar{h}) of the link CGH . Unknowns m and n are eliminated by subtracting the first equations of \mathcal{C}_1 and \mathcal{C}_2 from the rest of the equations in each set, respectively. Next, the unknowns are placed in seven sets of vectors

$$\begin{aligned}\mathbf{v}_j &= (C, d, R_j, R_1, 1), \quad j = 2, \dots, 8, \\ \mathbf{w}_j &= (C, f, R_j, R_1, 1), \quad j = 2, \dots, 8.\end{aligned} \quad (8)$$

Then, the synthesis equations can be written in the form,

$$\begin{aligned}\mathbf{v}_j^T [M_j] \bar{\mathbf{v}}_j &= 0 \\ &= \begin{pmatrix} C \\ d \\ R_j \\ R_1 \\ 1 \end{pmatrix}^T \begin{bmatrix} 0 & M_{1j} & M_{2j} & M_{3j} & M_{6j} \\ \bar{M}_{1j} & 0 & M_{4j} & M_{5j} & M_{7j} \\ \bar{M}_{2j} & \bar{M}_{4j} & 0 & 0 & M_{8j} \\ \bar{M}_{3j} & \bar{M}_{5j} & 0 & 0 & -M_{8j} \\ \bar{M}_{6j} & \bar{M}_{7j} & \bar{M}_{8j} & -\bar{M}_{8j} & 0 \end{bmatrix} \begin{pmatrix} \bar{C} \\ \bar{d} \\ \bar{R}_j \\ \bar{R}_1 \\ 1 \end{pmatrix}, \\ &\quad j = 2, \dots, 8,\end{aligned} \quad (9)$$

where

$$\begin{aligned}M_{1j} &= -\bar{Q}_j + \bar{Q}_1, \quad M_{2j} = g, \quad M_{3j} = -g, \\ M_{4j} &= -gQ_j, \quad M_{5j} = gQ_1, \quad M_{6j} = 0, \\ M_{7j} &= \bar{A}(Q_j - Q_1), \quad M_{8j} = -\bar{A}g,\end{aligned} \quad (10)$$

and

$$\begin{aligned}\mathbf{w}_j^T [N_j] \bar{\mathbf{w}}_j &= 0 \\ &= \begin{pmatrix} C \\ f \\ R_j \\ R_1 \\ 1 \end{pmatrix}^T \begin{bmatrix} 0 & N_{1j} & N_{2j} & N_{3j} & N_{6j} \\ \bar{N}_{1j} & 0 & N_{4j} & N_{5j} & N_{7j} \\ \bar{N}_{2j} & \bar{N}_{4j} & 0 & 0 & N_{8j} \\ \bar{N}_{3j} & \bar{N}_{5j} & 0 & 0 & -N_{8j} \\ \bar{N}_{6j} & \bar{N}_{7j} & \bar{N}_{8j} & -\bar{N}_{8j} & 0 \end{bmatrix} \begin{pmatrix} \bar{C} \\ \bar{f} \\ \bar{R}_j \\ \bar{R}_1 \\ 1 \end{pmatrix}, \\ &\quad j = 2, \dots, 8,\end{aligned} \quad (11)$$

where

$$\begin{aligned} N_{1j} &= -\bar{S}_j + \bar{S}_1, & N_{2j} &= \bar{h}, & N_{3j} &= -\bar{h}, \\ N_{4j} &= -\bar{h}S_j, & N_{5j} &= \bar{h}S_1, & N_{6j} &= 0, \\ N_{7j} &= \bar{B}(S_j - S_1), & N_{8j} &= -\bar{B}h. \end{aligned} \quad (12)$$

This results in 22 synthesis equations for the Watt II function generator where the first two sets of seven equations are obtained from the constraint equations (9) and (11), and the last set of eight are obtained from the normalization conditions (7). These equations have a bilinear structure,

$$\begin{aligned} \langle C, d, R_j, R_1, 1 \rangle \langle \bar{C}, \bar{d}, \bar{R}_j, \bar{R}_1, 1 \rangle, & \quad j = 2, \dots, 8, \\ \langle C, f, R_j, R_1, 1 \rangle \langle \bar{C}, \bar{f}, \bar{R}_j, \bar{R}_1, 1 \rangle, & \quad j = 2, \dots, 8, \\ \langle R_j, 1 \rangle \langle \bar{R}_j, 1 \rangle, & \quad j = 1, \dots, 8. \end{aligned} \quad (13)$$

For computation purposes, it is useful to divide the variables into the two groups,

$$\begin{aligned} \langle C, d, f, R_1, R_2, R_3, R_4, R_5, R_6, R_7, R_8 \rangle, \\ \langle \bar{C}, \bar{d}, \bar{f}, \bar{R}_1, \bar{R}_2, \bar{R}_3, \bar{R}_4, \bar{R}_5, \bar{R}_6, \bar{R}_7, \bar{R}_8 \rangle. \end{aligned} \quad (14)$$

The number of solutions to this system and the use of the Bertini software package in order to solve it is discussed in Section 5.

4.2 Stephenson II Synthesis Equations

The function generation problem of a Stephenson II linkage is to move its input link AC and its output link BDF through the angle pairs (ϕ_j, ψ_j) , $j = 1, \dots, 8$. The orientation of links AC , CGH , and BDF are given by angles ϕ_j , ρ_j , and ψ_j , respectively. The complex vector operators for each of these angles are Q_j , R_j , and S_j , respectively. The exponential definitions of these three operators and their conjugates appear in Eqn. 4. The conjugate pairs (Q_j, \bar{Q}_j) and (S_j, \bar{S}_j) are known from the accuracy points and (R_j, \bar{R}_j) is to be determined.

The loop equations are used to express links DG and FH ,

$$\begin{aligned} \mathcal{L}_1 : \quad G - D &= A + cQ_j + gR_j - B - dS_j, \\ \mathcal{L}_2 : \quad H - F &= A + cQ_j + hR_j - B - fS_j, \\ & \quad j = 1, \dots, 8. \end{aligned} \quad (15)$$

These links are constrained to the constant lengths $m = |G - D|$ and $n = |H - F|$, yielding the equations,

$$\begin{aligned} \mathcal{C}_1 : & (A + cQ_j + gR_j - B - dS_j) \\ & (\bar{A} + \bar{c}\bar{Q}_j + \bar{g}\bar{R}_j - \bar{B} - \bar{d}\bar{S}_j) = m^2, \\ \mathcal{C}_2 : & (A + cQ_j + hR_j - B - fS_j) \\ & (\bar{A} + \bar{c}\bar{Q}_j + \bar{h}\bar{R}_j - \bar{B} - \bar{f}\bar{S}_j) = n^2, \\ & \quad j = 1, \dots, 8. \end{aligned} \quad (16)$$

These 16 constraint equations along with the eight normalization conditions,

$$R_j \bar{R}_j = 1, \quad j = 1, \dots, 8, \quad (17)$$

yield 24 synthesis equations in the 24 unknowns (R_j, \bar{R}_j) and $(c, \bar{c}, d, \bar{d}, f, \bar{f}, m, n)$. Fixed pivots A and B are specified as well as the dimensions g and (h, \bar{h}) of link CGH . Unknowns m and n are eliminated by subtracting the first equations of \mathcal{C}_1 and \mathcal{C}_2 from the rest of the equations in each set, respectively. Next, the unknowns are placed in seven sets of vectors

$$\begin{aligned}\mathbf{v}_j &= (c, d, R_j, R_1, 1), \quad j = 2, \dots, 8, \\ \mathbf{w}_j &= (c, f, R_j, R_1, 1), \quad j = 2, \dots, 8.\end{aligned}\tag{18}$$

Then, the synthesis equations can be written in the form,

$$\begin{aligned}\mathbf{v}_j^T [M_j] \bar{\mathbf{v}}_j &= 0 \\ &= \begin{pmatrix} c \\ d \\ R_j \\ R_1 \\ 1 \end{pmatrix}^T \begin{bmatrix} 0 & M_{1j} & M_{2j} & M_{3j} & M_{6j} \\ \bar{M}_{1j} & 0 & M_{4j} & M_{5j} & M_{7j} \\ \bar{M}_{2j} & \bar{M}_{4j} & 0 & 0 & M_{8j} \\ \bar{M}_{3j} & \bar{M}_{5j} & 0 & 0 & -M_{8j} \\ \bar{M}_{6j} & \bar{M}_{7j} & \bar{M}_{8j} & -\bar{M}_{8j} & 0 \end{bmatrix} \begin{pmatrix} \bar{c} \\ \bar{d} \\ \bar{R}_j \\ \bar{R}_1 \\ 1 \end{pmatrix}, \\ &\quad j = 2, \dots, 8,\end{aligned}\tag{19}$$

where

$$\begin{aligned}M_{1j} &= -Q_j \bar{S}_j + Q_1 \bar{S}_1, \quad M_{2j} = g Q_j, \quad M_{3j} = -g Q_1, \\ M_{4j} &= -g S_j, \quad M_{5j} = g S_1, \quad M_{6j} = (\bar{A} - \bar{B})(Q_j - Q_1), \\ M_{7j} &= -(\bar{A} - \bar{B})(S_j - S_1), \quad M_{8j} = g(\bar{A} - \bar{B}),\end{aligned}\tag{20}$$

and

$$\begin{aligned}\mathbf{w}_j^T [N_j] \bar{\mathbf{w}}_j &= 0 \\ &= \begin{pmatrix} c \\ f \\ R_j \\ R_1 \\ 1 \end{pmatrix}^T \begin{bmatrix} 0 & N_{1j} & N_{2j} & N_{3j} & N_{6j} \\ \bar{N}_{1j} & 0 & N_{4j} & N_{5j} & N_{7j} \\ \bar{N}_{2j} & \bar{N}_{4j} & 0 & 0 & N_{8j} \\ \bar{N}_{3j} & \bar{N}_{5j} & 0 & 0 & -N_{8j} \\ \bar{N}_{6j} & \bar{N}_{7j} & \bar{N}_{8j} & -\bar{N}_{8j} & 0 \end{bmatrix} \begin{pmatrix} \bar{c} \\ \bar{f} \\ \bar{R}_j \\ \bar{R}_1 \\ 1 \end{pmatrix}, \\ &\quad j = 2, \dots, 8,\end{aligned}\tag{21}$$

where

$$\begin{aligned}N_{1j} &= -Q_j \bar{S}_j + Q_1 \bar{S}_1, \quad N_{2j} = \bar{h} Q_j, \quad N_{3j} = -\bar{h} Q_1, \\ N_{4j} &= -\bar{h} S_j, \quad N_{5j} = \bar{h} S_1, \quad N_{6j} = (\bar{A} - \bar{B})(Q_j - Q_1), \\ N_{7j} &= -(\bar{A} - \bar{B})(S_j - S_1), \quad N_{8j} = h(\bar{A} - \bar{B}).\end{aligned}\tag{22}$$

Eqns. 17, 19, and 21 form 22 synthesis equations of the form

$$\begin{aligned}\langle c, d, R_j, R_1, 1 \rangle \langle \bar{c}, \bar{d}, \bar{R}_j, \bar{R}_1, 1 \rangle, \quad j &= 2, \dots, 8, \\ \langle c, f, R_j, R_1, 1 \rangle \langle \bar{c}, \bar{f}, \bar{R}_j, \bar{R}_1, 1 \rangle, \quad j &= 2, \dots, 8, \\ \langle R_j, 1 \rangle \langle \bar{R}_j, 1 \rangle, \quad j &= 1, \dots, 8.\end{aligned}\tag{23}$$

The bilinear structure of the above equations allows us to place unknowns into the two groups,

$$\begin{aligned} & \langle c, d, f, R_1, R_2, R_3, R_4, R_5, R_6, R_7, R_8 \rangle, \\ & \langle \bar{c}, \bar{d}, \bar{f}, \bar{R}_1, \bar{R}_2, \bar{R}_3, \bar{R}_4, \bar{R}_5, \bar{R}_6, \bar{R}_7, \bar{R}_8 \rangle. \end{aligned} \quad (24)$$

The computation of solutions is described in Section 5.

4.3 Stephenson III Synthesis Equations

The task of the Stephenson III function generator is to coordinate links AD and BF according to the eight pairs of angles (ϕ_j, ψ_j) , $j = 1, \dots, 8$. Note that the input-output function between links AD and CG is not of interest because they both belong to the same four-bar loop. As well, when BF is the output link, the synthesis problem remains the same whether AD or CG is the input link.

Rotations by the angles ϕ_j , ρ_j , and ψ_j are implemented by the complex vector operators Q_j , R_j , and S_j , respectively. These operators and their conjugates are defined in Eqn. 4. The complex pairs (Q_j, \bar{Q}_j) and (S_j, \bar{S}_j) are known from the task specification and (R_j, \bar{R}_j) remain to be solved by the synthesis procedure.

Links CG and FH are expressed via the loop equations to yield

$$\begin{aligned} \mathcal{L}_1 : \quad G - C &= A + dQ_j + gR_j - C, \\ \mathcal{L}_2 : \quad H - F &= A + dQ_j + hR_j - B - fS_j, \end{aligned} \quad j = 1, \dots, 8. \quad (25)$$

These links are constrained to be the constant lengths $m = |G - C|$ and $n = |H - F|$. The squares of these lengths are expressed by multiplying \mathcal{L}_1 and \mathcal{L}_2 by their conjugates to attain,

$$\begin{aligned} \mathcal{C}_1 : (A + dQ_j + gR_j - C)(\bar{A} + \bar{d}\bar{Q}_j + \bar{g}\bar{R}_j - \bar{C}) &= m^2, \\ \mathcal{C}_2 : (A + dQ_j + hR_j - B - fS_j) & \\ (\bar{A} + \bar{d}\bar{Q}_j + \bar{h}\bar{R}_j - \bar{B} - \bar{f}\bar{S}_j) &= n^2, \end{aligned} \quad j = 1, \dots, 8. \quad (26)$$

By including the eight normalization conditions,

$$R_j \bar{R}_j = 1, \quad j = 1, \dots, 8, \quad (27)$$

we attain 24 synthesis equations in the 24 unknowns (R_j, \bar{R}_j) and $(C, \bar{C}, d, \bar{d}, f, \bar{f}, m, n)$. Fixed pivots A and B , and the dimensions g and (h, \bar{h}) of link CGH are specified. Unknowns m and n are eliminated by subtracting the first equations of \mathcal{C}_1 and \mathcal{C}_2 from the rest of the equations in each set, respectively. Next, the unknowns are placed in seven sets of vectors

$$\begin{aligned} \mathbf{v}_j &= (d, c, R_j, R_1, 1), \quad j = 2, \dots, 8, \\ \mathbf{w}_j &= (d, f, R_j, R_1, 1), \quad j = 2, \dots, 8. \end{aligned} \quad (28)$$

Then, the synthesis equations can be written in the form,

$$\begin{aligned} \mathbf{v}_j^T [M_j] \bar{\mathbf{v}}_j &= 0 \\ &= \begin{pmatrix} d \\ C \\ R_j \\ R_1 \\ 1 \end{pmatrix}^T \begin{bmatrix} 0 & M_{1j} & M_{2j} & M_{3j} & M_{6j} \\ \bar{M}_{1j} & 0 & M_{4j} & M_{5j} & M_{7j} \\ \bar{M}_{2j} & \bar{M}_{4j} & 0 & 0 & M_{8j} \\ \bar{M}_{3j} & \bar{M}_{5j} & 0 & 0 & -M_{8j} \\ \bar{M}_{6j} & \bar{M}_{7j} & \bar{M}_{8j} & -\bar{M}_{8j} & 0 \end{bmatrix} \begin{pmatrix} \bar{d} \\ \bar{C} \\ \bar{R}_j \\ \bar{R}_1 \\ 1 \end{pmatrix}, \\ &\quad j = 2, \dots, 8, \end{aligned} \quad (29)$$

where

$$\begin{aligned} M_{1j} &= -Q_j + Q_1, & M_{2j} &= gQ_j, & M_{3j} &= -gQ_1, \\ M_{4j} &= -g, & M_{5j} &= g, & M_{6j} &= \bar{A}(Q_j - Q_1), \\ M_{7j} &= 0, & M_{8j} &= \bar{A}g, \end{aligned} \quad (30)$$

and

$$\begin{aligned} \mathbf{w}_j^T [N_j] \bar{\mathbf{w}}_j &= 0 \\ &= \begin{pmatrix} d \\ f \\ R_j \\ R_1 \\ 1 \end{pmatrix}^T \begin{bmatrix} 0 & N_{1j} & N_{2j} & N_{3j} & N_{6j} \\ \bar{N}_{1j} & 0 & N_{4j} & N_{5j} & N_{7j} \\ \bar{N}_{2j} & \bar{N}_{4j} & 0 & 0 & N_{8j} \\ \bar{N}_{3j} & \bar{N}_{5j} & 0 & 0 & -N_{8j} \\ \bar{N}_{6j} & \bar{N}_{7j} & \bar{N}_{8j} & -\bar{N}_{8j} & 0 \end{bmatrix} \begin{pmatrix} \bar{d} \\ \bar{f} \\ \bar{R}_j \\ \bar{R}_1 \\ 1 \end{pmatrix}, \\ &\quad j = 2, \dots, 8, \end{aligned} \quad (31)$$

where

$$\begin{aligned} N_{1j} &= -Q_j \bar{S}_j + Q_1 \bar{S}_1, & N_{2j} &= \bar{h}Q_j, & N_{3j} &= -\bar{h}Q_1, \\ N_{4j} &= -\bar{h}S_j, & N_{5j} &= \bar{h}S_1, & N_{6j} &= (\bar{A} - \bar{B})(Q_j - Q_1), \\ N_{7j} &= -(\bar{A} - \bar{B})(S_j - S_1), & N_{8j} &= h(\bar{A} - \bar{B}). \end{aligned} \quad (32)$$

Eqns. 27, 29, and 31 form 22 synthesis equations of the form

$$\begin{aligned} \langle d, C, R_j, R_1, 1 \rangle \langle \bar{d}, \bar{C}, \bar{R}_j, \bar{R}_1, 1 \rangle, &\quad j = 2, \dots, 8, \\ \langle d, f, R_j, R_1, 1 \rangle \langle \bar{d}, \bar{f}, \bar{R}_j, \bar{R}_1, 1 \rangle, &\quad j = 2, \dots, 8, \\ \langle R_j, 1 \rangle \langle \bar{R}_j, 1 \rangle, &\quad j = 1, \dots, 8. \end{aligned} \quad (33)$$

The bilinear structure of the above equations allows us to place unknowns into the two groups,

$$\begin{aligned} \langle C, d, f, R_1, R_2, R_3, R_4, R_5, R_6, R_7, R_8 \rangle, \\ \langle \bar{C}, \bar{d}, \bar{f}, \bar{R}_1, \bar{R}_2, \bar{R}_3, \bar{R}_4, \bar{R}_5, \bar{R}_6, \bar{R}_7, \bar{R}_8 \rangle. \end{aligned} \quad (34)$$

The computation of solutions is described in the next section.

5 Solution of the Synthesis Equations

The synthesis equations for Watt II, Stephenson II and III function generators each yield a set of 22 equations in 22 unknowns of the form,

$$\begin{aligned}\mathbf{v}_j^T [M_j] \bar{\mathbf{v}}_j &= 0, \quad j = 2, \dots, 8, \\ \mathbf{w}_j^T [N_j] \bar{\mathbf{w}}_j &= 0, \quad j = 2, \dots, 8, \\ R_j \bar{R}_j - 1 &= 0, \quad j = 1, \dots, 8.\end{aligned}\tag{35}$$

The Bezout degree for a system of this form is $2^{22} = 4,194,304$. However, because the equations are bilinear, the General Linear Bound for this system is $\binom{22}{11} = 705,432$ [17] [18]. The synthesis equations are solved for the dimensions of the function generator by using the numerical homotopy software, Bertini. Numerical homotopy provides a standardized way to solve these equations [14, 19].

Numerical homotopy solves a polynomial system $P(\mathbf{z}) = 0$ by starting with the similar polynomial system $Q(\mathbf{z}) = 0$ with a known set of solutions. The system $Q(\mathbf{z})$ is transformed into $P(\mathbf{z})$ so the solutions of $Q(\mathbf{z}) = 0$ move to become the solutions of $P(\mathbf{z}) = 0$. This can be viewed as the numerical solution of a set of ordinary differential equations where the solutions of $Q(\mathbf{z}) = 0$ are the initial conditions.

To see how this is done, consider the array of polynomials $P(\mathbf{z})$ that form the loop equations of a linkage,

$$P(\mathbf{z}) = \begin{Bmatrix} S_1(\mathbf{z}) \\ S_2(\mathbf{z}) \\ \vdots \\ S_n(\mathbf{z}) \end{Bmatrix} = 0,\tag{36}$$

where $\mathbf{z} = (z_1, z_2, \dots, z_n)$ is the vector of unknowns. Now construct the convex combination homotopy map

$$H(\lambda, \mathbf{z}) = (1 - \lambda)Q(\mathbf{z}) + \lambda P(\mathbf{z}),\tag{37}$$

where $\lambda \in [0, 1]$ is the real-valued homotopy parameter. The coefficients of the polynomial system $P(\mathbf{z}) = 0$ are complex and its solutions \mathbf{z} are complex too. Therefore, the homotopy $H(\lambda, \mathbf{z})$ must be viewed as an array of n complex functions in n complex variables \mathbf{z} together with a single real variable λ .

For each root of the start system $Q(\mathbf{z}) = 0$, denoted $\mathbf{z} = \mathbf{a}_k$, $k = 1, \dots, N$, the homotopy equation $H(\lambda, \mathbf{z}) = 0$ has an associated zero curve γ_k , which is the connected component of $H^{-1}(0)$ containing the start point $(0, \mathbf{a}_k)$. The zero curve leads either to a point $(1, \mathbf{z}_k)$ where $P(\mathbf{z}_k) = 0$, or diverges to a root “at infinity.”

Along the zero curve γ_k , we have the identity $H(\gamma(s), \mathbf{z}(s)) = 0$, therefore we can compute

$$\frac{d}{ds} H(\lambda, \mathbf{z}) = [H_\lambda \quad H_{\mathbf{z}}] \begin{Bmatrix} d\lambda/ds \\ d\mathbf{z}/ds \end{Bmatrix} = 0.\tag{38}$$

where $[J_H] = [H_\lambda, H_{\mathbf{z}}]$ is the $n \times (n + 1)$ matrix of partial derivatives of the homotopy $H(\lambda, \mathbf{z})$. Notice that the vector $\mathbf{v} = (d\lambda/ds, d\mathbf{z}/ds)^T$ is tangent to the zero curve γ_k and is in the null space of the Jacobian matrix $[J_H]$. The zero curves are tracked numerically using predictor-corrector algorithms for solving ordinary differential equations [17].

Once a general solution is found for the synthesis equations for each case, parameter homotopy continuation is used to increase the efficiency of the computation [16] [14]. Parameter continuation is built into the Bertini software package. The idea behind parameter continuation is to solve Eqn. 35 via continuation with the 224 parameters of matrices $[M_j]$ and $[N_j]$, $j = 2, \dots, 8$ specified as random complex numbers. This includes specifying (M_{qj}, \bar{M}_{qj}) and (N_{qj}, \bar{N}_{qj}) such that they are not complex conjugate pairs. This one-time computation tracks

all 705,432 solutions and sorts out the 92,736 nonsingular, nondegenerate solutions. The randomly generated parameters are then used in conjunction with these nonsingular solutions to construct straight-line homotopies for (35) where matrices $[M_j]$ and $[N_j]$ are redefined for synthesis according to Eqns. 10 and 12, Eqns. 20 and 22, or Eqns. 30 and 32. The straight-line homotopies need only to track 92,736 paths. The time required to track all paths of the single generic homotopy took 107 minutes. The average computational time of the straight-line homotopies reported in this paper was 40 minutes. All computations were run in parallel on a Mac Pro with 12×2.93 GHz processors.

6 Analysis Equations

The solutions to the forward kinematics equations are used to find all the assembly configurations for a given input value ϕ . We formulate the forward kinematics for each of the three topologies individually. Note that since a six-bar mechanism consists of two kinematic loops, there are two computed joint parameters ρ and ψ for a single input value ϕ that completely describes a configuration. As well, for each value of ϕ , there will always be multiple values of ρ and ψ corresponding to different assembly configurations.

6.1 Watt II Analysis Equations

The constraint equations (6) that were used for the synthesis of the Watt II are also used to form its forward kinematics equations,

$$\begin{aligned} C_1(Q, \bar{Q}, R, \bar{R}) &= \\ (A + dQ - C - gR)(\bar{A} + \bar{d}\bar{Q} - \bar{C} - g\bar{R}) - m^2 &= 0, \\ C_2(Q, \bar{Q}, R, \bar{R}, S, \bar{S}) &= \\ (B + fS - C - hR)(\bar{B} + \bar{f}\bar{S} - \bar{C} - \bar{h}\bar{R}) - n^2 &= 0, \end{aligned} \quad (39)$$

together with the normalizing conditions,

$$\begin{aligned} N_1(R, \bar{R}) &= R\bar{R} - 1 = 0, \\ N_2(S, \bar{S}) &= S\bar{S} - 1 = 0. \end{aligned} \quad (40)$$

Note that the input angle ϕ is represented by (Q, \bar{Q}) and the configuration angles ρ and ψ are represented by (R, \bar{R}) and (S, \bar{S}) , respectively. All other parameters are known linkage dimensions.

Eqns. (39) and (40) form four bilinear equations in the unknowns (R, \bar{R}, S, \bar{S}) . Note that $\{C_1, N_1\}$ form a quadratic subsystem that can be solved independently for two solutions of (R, \bar{R}) . These solutions can be plugged into $\{C_2, N_2\}$ to form two more systems of two quadratic equations. Each of which has two solutions of (S, \bar{S}) for a total of four solutions for a single input pair (Q, \bar{Q}) .

6.2 Stephenson II Analysis Equations

The constraint equations (16) that were used for the synthesis of the Stephenson II are also used to form its forward kinematics equations,

$$\begin{aligned} C_1(Q, \bar{Q}, R, \bar{R}, S, \bar{S}) &= \\ (A + cQ + gR - B - dS)(\bar{A} + \bar{c}\bar{Q} + g\bar{R} - \bar{B} - \bar{d}\bar{S}_j) - m^2 &= 0, \\ C_2(Q, \bar{Q}, R, \bar{R}, S, \bar{S}) &= \\ (A + cQ + hR - B - fS)(\bar{A} + \bar{c}\bar{Q} + \bar{h}\bar{R} - \bar{B} - \bar{f}\bar{S}) - n^2 &= 0, \end{aligned} \quad (41)$$

along with the normalizing conditions (40) to form four bilinear equations in the unknowns (R, \bar{R}, S, \bar{S}) . McCarthy [18] uses an algebraic elimination procedure to solve equations of this form for the synthesis of a spherical RR

chain. His procedure results in a degree six polynomial resultant, the roots of which result in the dimensions of six RR chains. For the case of Eqns. 40 and 41, these roots represent six assembly configurations of a Stephenson II six-bar actuated from link *AC*.

It is important to note that in this paper we study Stephenson II function generators that move through the accuracy points (ϕ_j, ψ_j) , $j = 1, \dots, 8$, where ϕ is the input and ψ is the output. We do not analyze function generators that move through the inverse function where ψ is the input and ϕ is the output. Although for the latter case, the synthesis equations do not change, the analysis of a linkage is dependent upon which parameter is the input. The analysis routine presented in this paper focuses on the elimination of branch defects, and a mechanism's branches are dependent on which link is driven [20].

6.3 Stephenson III Analysis Equations

The forward kinematics equations are formed from the constraint equations (26) to yield

$$\begin{aligned} C_1(Q, \bar{Q}, R, \bar{R}) &= \\ (A + dQ + gR - C)(\bar{A} + \bar{d}\bar{Q} + g\bar{R} - \bar{C}) - m^2 &= 0, \\ C_2(Q, \bar{Q}, R, \bar{R}, S, \bar{S}) &= \\ (A + dQ + hR - B - fS)(\bar{A} + \bar{d}\bar{Q} + \bar{h}\bar{R} - \bar{B} - \bar{f}\bar{S}) - n^2 &= 0, \end{aligned} \quad (42)$$

Combining these equations with the normalizing conditions (40) forms four bilinear equations in the unknowns (R, \bar{R}, S, \bar{S}) . The solution of which follows that of the Watt II forward kinematics equations, resulting in four solutions corresponding to four assembly configurations.

Similar to the Stephenson II case, we have neglected analyzing Stephenson III function generators actuated with ψ as the input and ϕ as the output, despite having synthesis equations identical to those presented in this paper. Also note that the synthesis and analysis procedures are the same whether *AD* or *CG* is the input link and *BF* is the output link.

7 Analysis Procedure

The objective of this analysis is to determine whether the linkage solutions generated by Bertini are capable of producing a smooth trajectory that moves the input and output links through all required accuracy points. Our notion of a smooth trajectory is defined as a continuous set of configurations that does not pass through a singular point, what others have referred to as a mechanism branch [20] [21].

Prior to this analysis, linkage solutions that are not physically realizable or that contain particularly small link lengths are sorted out. The condition for a solution to be physically realizable is that the two variable groups (14) (24) (34) solved for need to be complex conjugates of each other. The large majority of solutions found are not physically realizable. As well, solutions in which the magnitude of C , d , or f was found to be less than or equal to 0.005 were removed in order to limit solutions with particularly small link lengths.

In this section, we examine all the mechanism branches a linkage is capable of producing, and determine whether or not it achieves the desired accuracy points. Mechanism branches are pieced together by solving the forward kinematics equations as presented in Section 6 for all assembly configurations for a series of input angles ϕ that represent a full revolution of the input link. Each configuration is sorted into a trajectory according to a sorting algorithm. These trajectories represent mechanism branches.

7.1 Sorting Assembly Configurations

In order to determine the movement of a six-bar linkage, the forward kinematics equations are solved for an array of input angles ϕ_k to obtain $\rho_{k,l}$ and $\psi_{k,l}$, where $l = 1, \dots, 6$ identifies the configurations for that input angle. As ϕ_k is incremented, the solutions to these equations do not appear in any order. It is the goal of this section to sort each configuration $(\phi_k, \rho_{k,l}, \psi_{k,l})$ into a smooth trajectory curve.

The input of a mechanism at position k is defined as a vector \mathbf{x}_k and the output as a vector $\mathbf{y}_{k,l}$, such that

$$\mathbf{x}_k = \begin{pmatrix} Q_k \\ \bar{Q}_k \end{pmatrix} \quad \text{and} \quad \mathbf{y}_{k,l} = \begin{pmatrix} R_{k,l} \\ S_{k,l} \\ \bar{R}_{k,l} \\ \bar{S}_{k,l} \end{pmatrix}, \quad l = 1, \dots, 6. \quad (43)$$

The vector \mathbf{F} is formed such that

$$\mathbf{F}(\mathbf{x}, \mathbf{y}) = \begin{Bmatrix} C_1(\mathbf{x}, \mathbf{y}) \\ C_2(\mathbf{x}, \mathbf{y}) \\ N_1(\mathbf{y}) \\ N_2(\mathbf{y}) \end{Bmatrix} = \begin{Bmatrix} 0 \\ 0 \\ 0 \\ 0 \end{Bmatrix}, \quad (44)$$

where the kinematics equations $\{C_1, C_2\}$ are defined in (39), (41), or (42) and $\{N_1, N_2\}$ are defined in (40). The Jacobian of this function is

$$[J_{\mathbf{F}}] = \left[\frac{\partial \mathbf{F}}{\partial R}, \frac{\partial \mathbf{F}}{\partial S}, \frac{\partial \mathbf{F}}{\partial \bar{R}}, \frac{\partial \mathbf{F}}{\partial \bar{S}} \right] \quad (45)$$

The objective of this algorithm at an input step k is to connect each configuration from set \mathcal{A} to a configuration in set \mathcal{B} where

$$\mathcal{A} = \{(\mathbf{x}_k, \mathbf{y}_{k,l}) \mid l = 1, \dots, 6\} \quad (46)$$

and

$$\mathcal{B} = \{(\mathbf{x}_{k+1}, \mathbf{y}_{k+1,p}) \mid p = 1, \dots, 6\}. \quad (47)$$

Note that in general a connecting pair will have $l \neq p$. In order to connect each pair, the Taylor series expansion of the kinematics equations is used at position $k + 1$ given by

$$\mathbf{F}(\mathbf{x}_{k+1}, \mathbf{y}_{k+1,l}) \approx \mathbf{F}(\mathbf{x}_{k+1}, \mathbf{y}_{k,l}) + [J_{\mathbf{F}}]_k (\mathbf{y}_{k+1,l} - \mathbf{y}_{k,l}). \quad (48)$$

In order to estimate the value of $\mathbf{y}_{k+1,l}$ that yields $\mathbf{F} = 0$, the approximate values $\tilde{\mathbf{y}}_{k+1,l}$ are computed,

$$\tilde{\mathbf{y}}_{k+1,l} = \mathbf{y}_{k,l} - [J_{\mathbf{F}}]_k^{-1} \mathbf{F}(\mathbf{x}_{k+1}, \mathbf{y}_{k,l}), \quad l = 1, \dots, 6 \quad (49)$$

These values form the set $\tilde{\mathcal{B}}$ of approximations where

$$\tilde{\mathcal{B}} = \{(\mathbf{x}_{k+1}, \tilde{\mathbf{y}}_{k+1,l}) \mid l = 1, \dots, 6\}. \quad (50)$$

If the l^{th} element of $\tilde{\mathcal{B}}$ is sufficiently close to the p^{th} element of \mathcal{B} , then the p^{th} element of \mathcal{B} is taken as the neighbor of the l^{th} element of \mathcal{A} on a smooth trajectory. Once each element of \mathcal{A} is connected to a element of \mathcal{B} , the algorithm increments to the next step. Cases in which one to one correspondence do not occur are described in the following section.

7.2 Identifying Branch Points

The technique described above for sorting the roots of the kinematics equations among assembly configurations can fail at singular and near-singular configurations. That is where

$$\det[J_F(\mathbf{x}_k, \mathbf{y}_{k,l})] \approx 0. \quad (51)$$

Near singular configurations can be present even if there is no singularity in the vicinity. Near singular cases are troublesome because the tracking algorithm can jump from one smooth trajectory to another.

Unlike other methods that explicitly solve for all singular points beforehand [22], our algorithm attempts to sort through the singular points with no prior knowledge to their location. Because singularities mark the input limits of a mechanism, our algorithm sorts configurations whether or not they are entirely physically realizable.

In particular, the tracked curves consist of the elements (R, S, \bar{R}, \bar{S}) parameterized by ϕ . The behavior of curves in this space is related to the behavior of curves in a similar space shown in Fig. 2. This figure plots the real and imaginary components of the output S against the independent input parameter ϕ . Configurations are physically realizable at locations where $|S| = 1$, that is where the curves lie on the cylinder. Computed singular locations are marked with purple dots. Note that the curves in Fig. 2 can cross at nonsingular locations because this graph does not include information about R . However, in the higher dimensional configuration space, curves only cross at singular points.

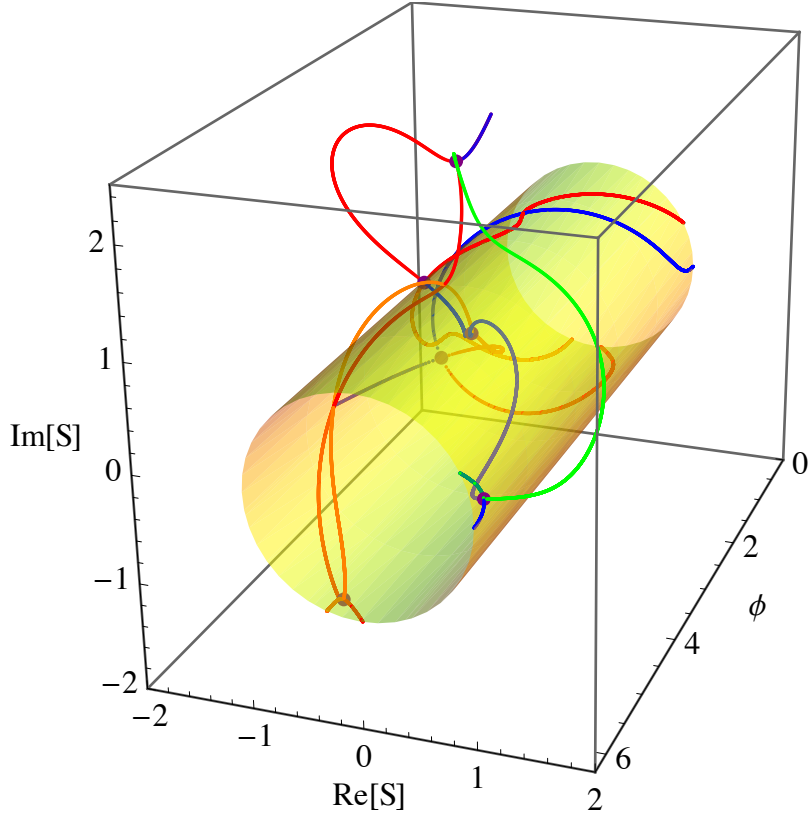


Fig. 2. Example of branch sorting and the presence of singularities.

It is near singularities that the algorithm can fail to find a one to one correspondence between sets \mathcal{A} and \mathcal{B} described in Eqns. 46 and 47. Logic is used to address this issue. The set \mathcal{A} contains the last elements of the trajectories arriving at position k , and \mathcal{B} contains the first elements of the trajectories departing from position $k + 1$. At each position we apply the following logic:

1. If each element of \mathcal{A} connects uniquely to an element of \mathcal{B} , the algorithm moves on to the next position;
2. If an element of \mathcal{B} is not connected to an element of \mathcal{A} , that element of \mathcal{B} begins a new trajectory;
3. If an element of \mathcal{A} connects to multiple elements of \mathcal{B} , the trajectory associated with that element of \mathcal{A} is duplicated and each duplicate connects to a matching element of \mathcal{B} ;
4. If an element of \mathcal{A} does not connect to an element of \mathcal{B} , the trajectory associated with that element of \mathcal{A} is concluded.

Physically realizable sections are separated out upon conclusion of the path tracking algorithm. These sections are then split at points where the sign of the Jacobian determinant changes in order to find cases where the algorithm may jump between trajectories. It is possible for such a jump between trajectories to occur without change in sign of the Jacobian [20]. Our algorithm cannot detect these jumps.

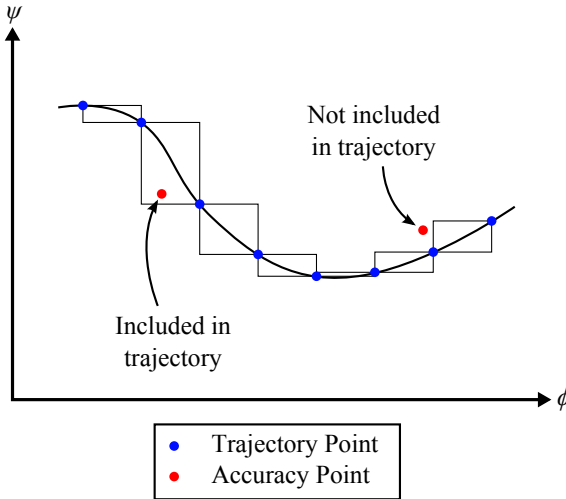


Fig. 3. Criterion used for determining whether a trajectory contains an accuracy point.

7.3 Determining Useful Designs

Once a six-bar function generator has been designed and mechanism branches have been constructed, it is next determined how many accuracy points lie on a single branch trajectory. Ideally, we prefer to find trajectories that pass through all eight accuracy points. However, we have found that trajectories that pass through seven points and six points can be of practical use as well. Therefore we enumerate all these mechanisms and leave them for the designer's review.

In order to determine that an accuracy point is on a trajectory, we must decide if the accuracy point is within a specified distance of the list of points that define a trajectory. To do this it is determined whether an accuracy point is contained in a box defined by two neighboring trajectory points in the ϕ - ψ plane as shown in Fig. 3. Note that six-bar linkages with non-zero error at the accuracy points can satisfy this criterion.

8 Svoboda's Logarithm Linkage

In this section, our design methodology is verified by solving for Watt II six-bar linkages that generate the logarithm function generated by Svoboda's patented design. Figure 4(a) shows his “double three-bar” linkage, which is now called a Watt II six-bar linkage. The function that Svoboda mechanized is given by,

$$x_2 = \log_{10} x_1, \quad 1 \leq x_1 \leq 50. \quad (52)$$

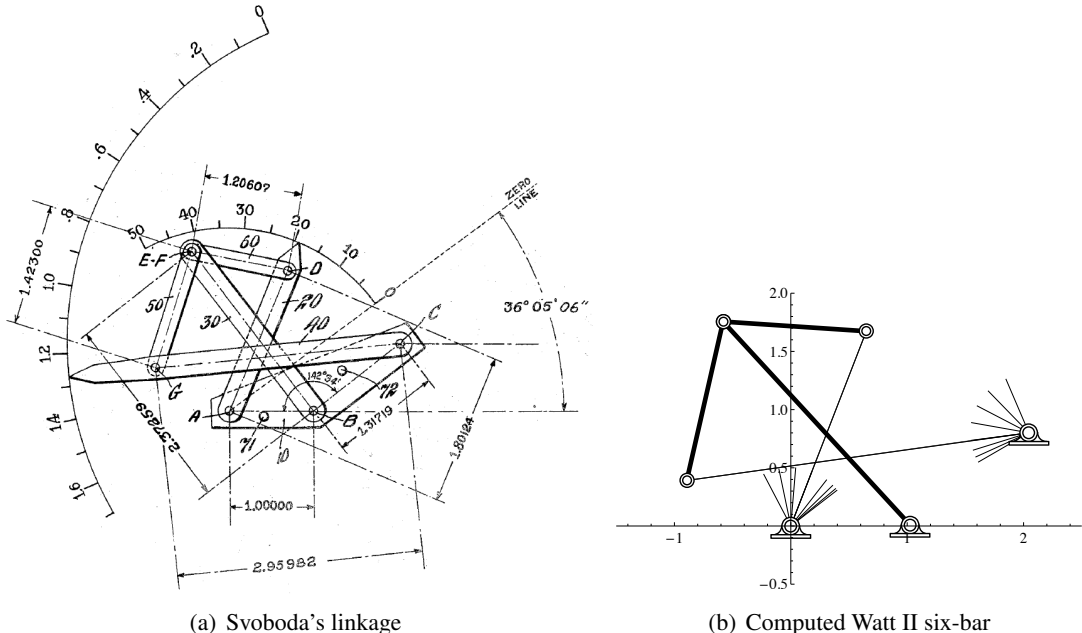


Fig. 4. Comparison of Svoboda's logarithm linkage (U.S. Patent 2340350, Feb. 1, 1944) and the computed Watt II six-bar linkage.

He introduced the following scaling so that the variables x_1 and x_2 could be read from the input and output angles, ϕ and ψ , of the linkage,

$$\begin{aligned}\phi_{\min} &= 36.08500000 < \phi < \phi_{\max} = 117.63333333 \\ \psi_{\min} &= 113.16981735 < \psi < \psi_{\max} = 210.05171929.\end{aligned}\quad (53)$$

The result is the function,

$$\psi = \frac{\Psi_{\max} - \Psi_{\min}}{\log_{10} 50} \log_{10} \left(\frac{50 (\phi - \phi_{\min})}{\phi_{\max} - \phi_{\min}} \right) + \Psi_{\min}. \quad (54)$$

Our goal is to find the Watt II six-bar linkages that fit this function at eight accuracy points, Table 9.

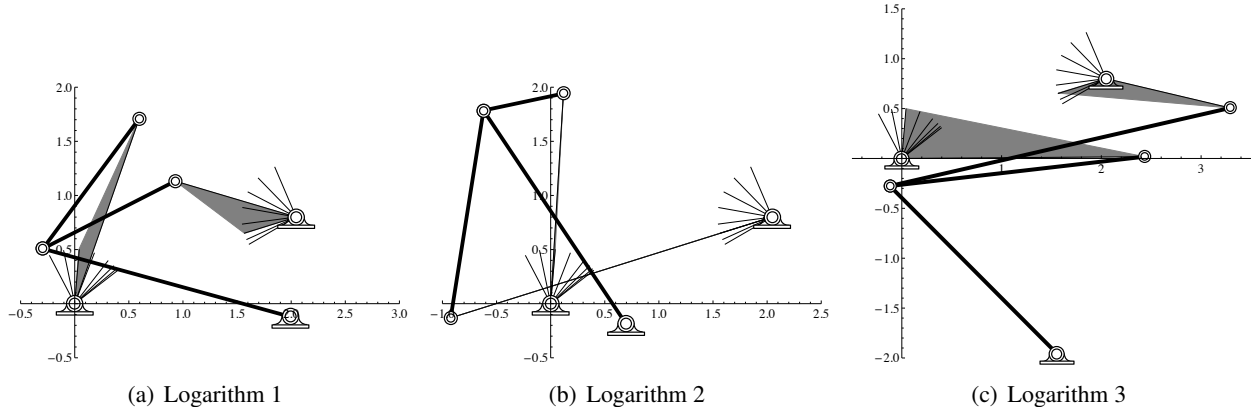


Fig. 5. Three more Watt II six-bar linkages that fit the eight accuracy points of Svoboda's logarithmic function. Each linkage is displayed in the sixth accuracy position.

Bertini's parameter homotopy followed 92,736 paths to obtain 29,395 nonsingular solutions. Of these, only 65 were linkages found that passed through all eight accuracy points without a branch defect. A summary of

Table 1. (a) Accuracy points and (b) specified dimensions attained from Svoboda's linkage design. Points were specified up to 8 decimal digits.

(a) Accuracy points		
j	ϕ_j	ψ_j
1	37.71666667°	113.16981735°
2	39.80000000°	134.21966883°
3	44.10000000°	152.52871342°
4	52.20000000°	169.93900165°
5	68.80000000°	187.47879093°
6	85.20000000°	197.28493451°
7	101.80000000°	204.41742081°
8	117.63333333°	210.05171929°

(b) Specified dimensions	
A	0+0 <i>i</i>
B	2.04592938+0.80063801 <i>i</i>
g	2.37259+0 <i>i</i>
h	2.37259+0 <i>i</i>

Table 2. Computation information for Svoboda's logarithm function.

Nonsingular Solutions	29,395
Physically Realizable Solutions	953
8-Point Mechanisms	65
7-Point Mechanisms	81
6-Point Mechanisms	136
Synthesis Computation Time	45 min
Analysis Computation Time	84 min
Analysis Timeouts	0
Analysis Resolution	0.18009°

the computational information is provided in Table 2. As noted by McLarnan [9], linkages that may be defective can be useful if they have seven, even six accuracy points on a single branch, which yields an additional 81 and 136 linkage designs, respectively.

A comparison of these linkages to Svoboda's linkage shows that one of the 65 linkages that reach all eight accuracy points has similar dimensions, Fig. 4. Table 8 shows that the differences between the dimensions that define Svoboda's mechanical computer and our six-bar linkage are less than 3%. Figure 5 presents three other Watt II six-bar linkages that fit the eight accuracy points of Svoboda's logarithm function.

Table 3. Comparison of Svoboda's design and design found by our algorithm.

Dim.	Original	Computed	Percent Difference
C	1+0 <i>i</i>	1.02430996+0.01025573 <i>i</i>	2.64%
d	1.80124+0 <i>i</i>	1.79466456−0.00510634 <i>i</i>	0.46%
f	2.95982+0 <i>i</i>	2.96851339+0.01689144 <i>i</i>	0.64%
m	1.20607+0 <i>i</i>	1.23350280+0 <i>i</i>	2.27%
n	1.42300+0 <i>i</i>	1.40068248+0 <i>i</i>	1.57%

9 Comparison of Six-bars for Three Different Functions

In this section, the design of Watt II, Stephenson II and III function generators is carried out for three different task functions. The three functions examined are (i) a parabolic function used by McLarnan [9], (ii) a range ballistic function, and (iii) an elevation ballistic function. The ballistic functions were adapted from an example provided by Svoboda [5].

In each case, the number of defect-free linkages is determined that fit all eight accuracy points, as well as those that have seven and six accuracy points on a single branch. Examples of these designs are provided to illustrate the results.

Table 4. Accuracy points and dimensions specified for the parabolic function generator. For these calculations 300 decimal digits were used.
 (a) Accuracy points

j	ϕ_j	Ψ_j
1	0°	0°
2	15°	2.5°
3	30°	10°
4	44°	21.511111°
5	57°	36.1°
6	69°	52.9°
7	80°	71.111111°
8	90°	90°

(b) Specified dimensions

A	$0+0i$
B	$1+0i$
g	$0.333333+0i$
h	$0.166667+0.28867514i$

9.1 Parabolic Function

In this example, designs for Watt II, Stephenson II and III function generators are found for a parabolic function defined by the equation,

$$\Psi = \frac{1}{90}\phi^2, \quad (55)$$

where ϕ is the input angle and ψ is the output angle. The function is approximated by choosing eight accuracy points. Specified linkage dimensions are shown in Table 4.

Bertini's parameter homotopy was run for 92,736 paths to obtain 22,987, 64,078 and 45,763 nonsingular solutions, respectively, for the Watt II, Stephenson II and III six-bar function generators, Table 5. For the three cases, there were 86, 19 and 73 useful linkages that achieved the eight accuracy points. Thus, for this function one useful six-bar linkage was found for every 1078, 4881, and 1270 homotopy paths, respectively.

An example design from each topology is shown in Fig. 6. Also shown is a comparison of the specified function and the linkage input-output function with the difference between these functions amplified by 10,000. The largest deviation from the specified function among these three example linkages is found to be 0.025° in Fig. 6(f).

Examination of the error curve produced by the Watt II design (Fig. 6(b)) shows that the error at the fourth accuracy point is not zero, indicating that the displayed trajectory does not pass exactly through this accuracy point. It is actually the case that this linkage has a different branch that does contain the fourth accuracy point. This shows the susceptibility of computational synthesis to numerical error. In this case, two linkage branches are separated by only 0.0025 degrees of the accuracy point.

Table 5. Computation information for synthesis of the parabolic function generators.

	Watt II	Steph. II	Steph. III
Nonsingular Solutions	22,987	64,078	45,763
Realizable Solutions	493	141	600
8-Point Mechanisms	86	19	73
7-Point Mechanisms	97	20	113
6-Point Mechanisms	95	18	86
Synthesis Comp. Time	37 min	34 min	33 min
Analysis Comp. Time	19 min	24 min	30 min
Analysis Timeouts	0	12	0
Analysis Resolution	0.36036°	0.36036°	0.36036°

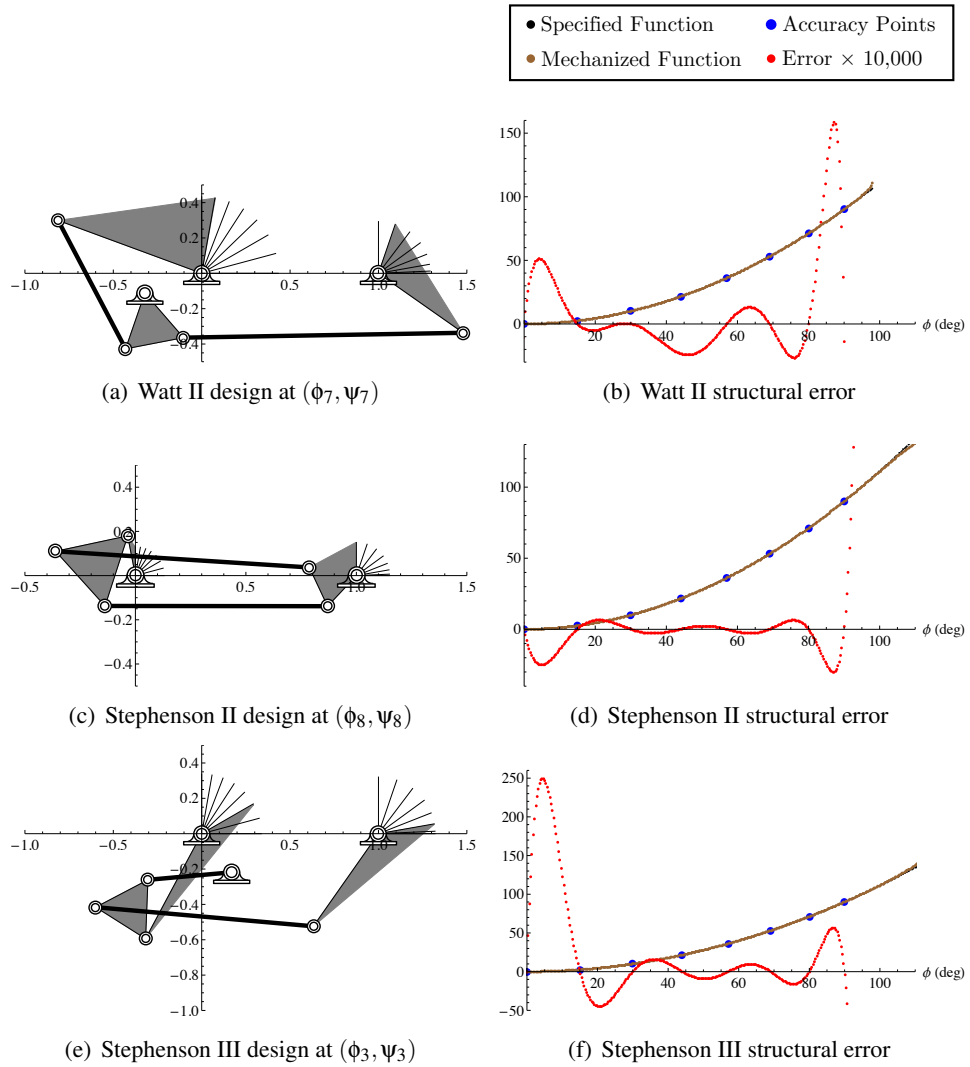


Fig. 6. Design options for the parabolic function for each topology.

9.2 Range Ballistic Function

Svoboda [5] provides a two degree of freedom linkage that computes the elevation of a gun to hit a target at a given distance and altitude. We separate this into two functions, (i) the range ballistic function that computes the

gun elevation angle to reach a given distance at zero altitude, and (ii) the elevation ballistic function to reach an altitude at a given range. These calculations assume the muzzle velocity of the artillery round is $v_0 = 500$ m/s and there is no air resistance so that the trajectory is a parabola.

The range ballistic function is designed so that the range scales linearly with the input angle ϕ such that $\phi = 0^\circ$ is set to 4000 m, and $\phi = 225^\circ$ is set to 25,484.2 m. The result is the range ballistic function,

$$\psi = 45^\circ - \frac{1}{2} \arccos \left(-\frac{g}{v_0^2} \left(\frac{(25,484.2 - 4000)\phi}{225} + 4000 \right) \right), \quad (56)$$

where g is the gravitational constant. This function is approximated by choosing eight accuracy points. Specified linkage dimensions are shown in Table 6.

Table 6. The eight accuracy points and specified dimensions for the range ballistic function. Values were specified up to 300 decimal digits.

(a) Accuracy points

j	ϕ_j	ψ_j
1	0°	4.5152437790°
2	40°	8.9342612197°
3	80°	13.5874276442°
4	115°	18.0021905273°
5	150°	22.9854405071°
6	185°	29.1127003302°
7	210°	35.3496863870°
8	224°	42.5192890583°

(b) Specified dimensions

A	$0 - 1i$
B	$0 + 0i$
g	$0.5 + 0i$
h	$0.25 + 0.4330127019i$

Bertini's parameter homotopy was run for 92,736 paths and yielded 1, 0 and 15 Watt II, Stephenson II and III six-bar function generators that reach eight accuracy points, Table 7. Thus, useful Watt II and Stephenson II linkages with eight accuracy points for this function were rare. A useful Stephenson III six-bar linkage was found for every 6,182 homotopy paths. Furthermore, examination of each design revealed link lengths of unacceptable dimensions, either too long or too short.

Figure 7 shows a Stephenson III linkage design that reached seven accuracy points. Although the designed linkage reaches only seven accuracy points $j = 2, \dots, 8$, it does pass close to the remaining accuracy point. A video of this linkage is available at <http://www.mechanicaldesign101.com>. This is another example of the numerical sensitivity of the computational synthesis process.

9.3 Elevation Ballistic Function

The elevation ballistic function sets the elevation angle of a gun so that a ballistic round reaches a specific altitude at a given range, in this case 15,000 m. The function was constructed so that the input angle ϕ is directed at the target, and the elevation of the gun is the output angle ψ , as shown in Fig. 8. This elevation ballistic function is given by

$$\psi = 45^\circ + \frac{1}{2}\phi - \frac{1}{2} \arccos \left(-\frac{15,000 g}{v_0^2} \cos \phi + \sin \phi \right). \quad (57)$$

This function is approximated with eight accuracy points. Specified dimensions are shown in Table 8. Several useful designs were found for all topologies. A Stephenson II design is shown in Figure 9.

Table 7. Computation information for synthesis of the range ballistic function generators.

	Watt II	Steph. II	Steph. III
Nonsingular Solutions	23,052	63,753	45,992
Realizable Solutions	891	3,497	1,920
8-Point Mechanisms	1	0	15
7-Point Mechanisms	40	16	77
6-Point Mechanisms	80	78	140
Synthesis Comp. Time	35 min	31 min	37 min
Analysis Comp. Time	36 min	340 min	126 min
Analysis Timeouts	0	1	3
Analysis Resolution	0.36036°	0.36036°	0.36036°

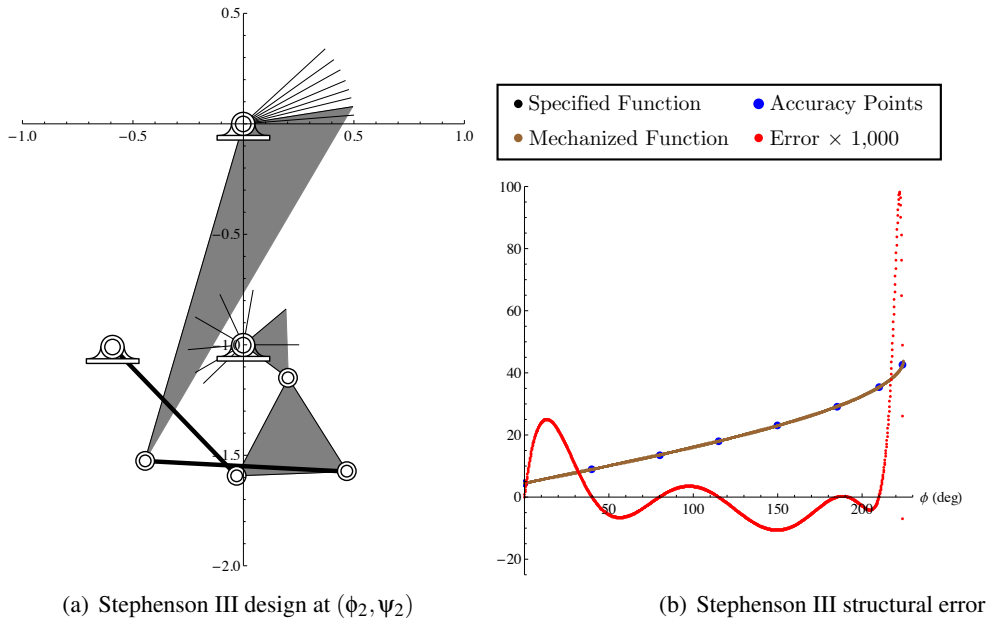


Fig. 7. Design options for the ballistic function.

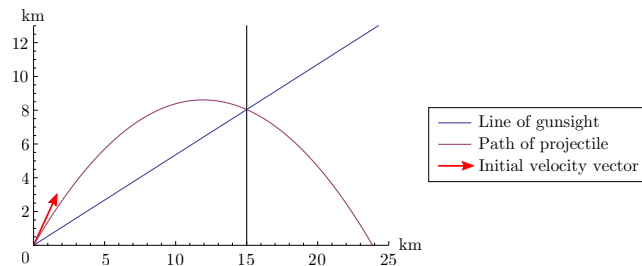


Fig. 8. The line of the gunsight and the parabolic path of the projectile intersect at a horizontal distance of 15 km.

Bertini's parameter homotopy was run for 92,736 paths to obtain 83, 125 and 92 useful Watt II, Stephenson II and III six-bar function generators that pass through the eight accuracy points shown in Table 9(a). This shows that a useful linkage was found in one out of 1117, 742 and 1008 homotopy paths, respectively.

Table 8. The eight accuracy points and specified dimensions for the ballistic function. Values were specified up to 300 decimal digits.
 (a) Accuracy points

j	ϕ_j	Ψ_j
1	0°	18.0288613860°
2	5°	23.6695051767°
3	10°	29.4387864830°
4	14°	34.1969096229°
5	18°	39.1602575004°
6	22°	44.4884326438°
7	26°	50.6650944462°
8	29°	58.7006824116°

(b) Specified dimensions

A	$0-1i$
B	$0+0i$
g	$0.5+0i$
h	$0.25+0.4330127019i$

Table 9. Computation information for the elevation ballistic function generators.

	Watt II	Steph. II	Steph. III
Nonsingular Solutions	21,315	60,680	42,691
Realizable Solutions	1,785	2,739	2,077
8-Point Mechanisms	83	125	92
7-Point Mechanisms	773	473	691
6-Point Mechanisms	415	809	502
Synthesis Comp. Time	45 min	48 min	50 min
Analysis Comp. Time	71 min	266 min	114 min
Analysis Timeouts	3	76	18
Analysis Resolution	0.36036°	0.36036°	0.36036°

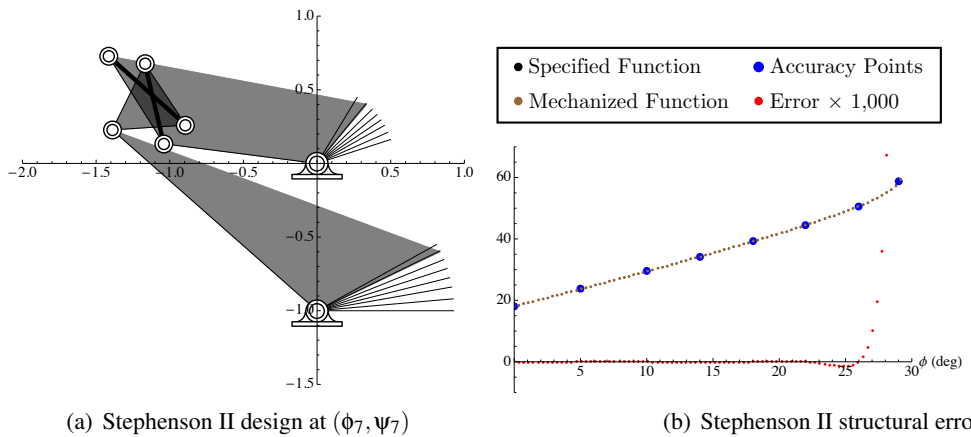


Fig. 9. Design options for the ballistic function.

10 Summary of Results

The study of the computational synthesis of useful Watt II, Stephenson II and Stephenson III six-bar linkages shows that there is a wide variation in number of nonsingular solutions needed per useful design. It is shown

from the synthesis exercises carried out above that the probability of finding a mechanism that passes through six, seven, or eight accuracy points from the nonsingular solutions supplied by Bertini is 1:97, 1:615 and 1:133 for the Watt II, Stephenson II and III designs, respectively.

The computation time needed to find and analyze each linkage type varied widely as well. It can be seen that the design and analysis of Stephenson II linkages takes more time than the other two types of linkages for these three functions. The Watt II and Stephenson III computation times ranged from 0.9 and 1.1 hrs, respectively, for the parabolic function, and from to 1.9 and 2.7 hrs for the elevation ballistic function. In contrast, the computation time for the Stephenson II was 1.0, 6.2 and 5.2 hrs for the three functions. These computations were performed in parallel on a Mac Pro with 12×2.93 GHz processors.

11 Conclusion

This paper examines the synthesis of Watt II, Stephenson II and Stephenson III six-bar linkages that generate a specified function using eight accuracy points, together with performance verification. This problem was originally formulated in 1963 (McLarnan [9]), but the computational resources needed were not available until 1994 (Dhingra et al. [10]). Complete solution of this problem requires not just solution of the synthesis equations but verification that the eight accuracy points lie on one branch. Our results yield a parameter homotopy that tracks 92,736 paths for the eight accuracy point synthesis problem for Watt II, Stephenson II or III six-bar linkages, evaluates the nonsingular solutions to identify physical linkages, and then evaluates each physical linkage to verify performance.

Three examples were presented: i) a parabolic function, ii) a range ballistic function, and iii) an elevation ballistic function. For each of the three functions, the Watt II synthesis equations yielded 493, 891, and 1785 physical linkages, respectively, of which only 86, 1, and 83 were nonbranching designs. Thus, the probability that any particular path of the homotopy will yield a useful linkage is less than one in a thousand. Similar results were obtained for the Stephenson II and Stephenson III linkages. The complete design calculation for a particular six-bar linkage type requires approximately 2 hours on a Mac Pro with 12×2.93 GHz processors.

References

- [1] Hartenberg, R. S., and Denavit, J.: *Kinematic Synthesis of Linkages*, New York: McGraw-Hill, 1964.
- [2] Kinzel, E. C., Schmiedeler, J. P. and Pennock, G. R.: “Function generation with finitely separated precision points using geometric constraint programming”, *J. Mechanical Design*, **129**, 1185, (2007).
- [3] Plecnik, M. M. and McCarthy, J. M.: “Five Position Synthesis of a Slider-Crank Function Generator”, In: Proceedings of the 2011 International Design Engineering Technical Conferences DETC2011-47581, Washington, D.C. (2011)
- [4] Bum Seok Kim, Hong Hee Yoo, “Unified synthesis of a planar four-bar mechanism for function generation using a spring-connected arbitrarily sized block model,” *Mechanism and Machine Theory*, Volume 49, March 2012, Pages 141-156, ISSN 0094-114X, <http://dx.doi.org/10.1016/j.mechmachtheory.2011.10.013>.
- [5] Svoboda, A.: *Computing mechanisms and linkages*, McGraw-Hill, New York, 1948. Available through Dover Publications, New York, 1965.
- [6] Wen-Min Hwang and Yi-Jie Chen, “Defect-free Synthesis of Stephenson-II Function Generators,” *Journal of Mechanisms and Robotics*, No. 041012, November 2012, Vol. 2.
- [7] A. Svoboda, inventor, U. S. Patent No. 2,340,350, “Mechanism for Use in Computing Apparatus,” Feb. 1, 1944.
- [8] Freudenstein, F. “An analytical approach to the design of four-link mechanisms”, *ASME Journal of Engineering for Industry Series B*, **76**(3), (1954).
- [9] C. W. McLarnan, “Synthesis of Six-Link Plane Mechanisms by Numerical Analysis,” *Journal of Engineering for Industry*, February 1963, pp. 5-10.
- [10] A. K. Dhingra, J. C. Cheng, and D. Kohli, “Synthesis of Six-link, Slider-crank and Four-link Mechanisms for Function, Path and Motion Generation Using Homotopy with m-homogenization,” *Journal of Mechanical Design*, Vol. 116, December 1994, pp. 1122-1131.

- [11] Sancibrian, R.: “Improved CRG method for the optimal synthesis of linkages in function generation problems,” *Mechanism and Machine Theory*, **46**, 1350-1375. (2011)
- [12] Wampler, C. W., Sommese, A. J., and Morgan, A. P.: “Complete Solution of the Nine-Point Path Synthesis Problem for Four-Bar Linkages”, *J. Mechanical Design*, 114(1) : 153-159 (1992)
- [13] Wampler, C. W.: “Isotropic Coordinates, Circularity, and Bezout Numbers: Planar Kinematics from a New Perspective”, *Proc. ASME 1996 Design Engineering Technical Conferences*, Paper No. 96-DETC/MECH-1210, Irvine, CA, (1996)
- [14] Sommese, A. J., and Wampler, C. W.: *The Numerical Solution of Systems of Polynomials Arising in Engineering and Science*, World Scientific Publ. Co. (2005).
- [15] Erdman, A. G., Sandor, G. N., and Kota, S.: *Mechanism Design: Analysis and Synthesis*, Prentice-Hall, 688p. (2001).
- [16] Morgan, A. P. and Sommese, A. J.: “Coefficient-parameter polynomial continuation”, *Applied Mathematics and Computations*, Volume 29, Issue 2, January 1989, Pages 123-160 (1989)
- [17] H. Su, J. M. McCarthy, M. Sosonkina, and L. T. Watson, “POLSYS_GLP: A Parallel General Linear Product Homotopy Code,” *ACM Trans. on Mathematical Software*, 32(4):561-579, December, 2006.
- [18] McCarthy, J. M. and Soh, G. S.: *Geometric Design of Linkages*, 2nd Ed., Springer-Verlag, (2010).
- [19] J Verschelde, “Algorithm 795: PHCpack: A General-Purpose Solver for Polynomial Systems by Homotopy Continuation,” *ACM Trans Mathematical Software* 25(2):251-276, 1999.
- [20] Chase, T. R. and Mirth, J. A.: “Circuits and Branches of Single-Degree-of-Freedom Planar Linkages”, *J. Mechanical Design*, **115**, 223–230, (1993).
- [21] Larochelle, P. R.: “Circuit and Branch Rectification of the Spatial 4C Mechanism”, In: Proceedings of the 2000 Design Engineering Technical Conferences DETC2000/MECH-14053, Baltimore, MD (2000)
- [22] Myszka, D. H., Murray, A. P., and Wampler, C. W.: “Mechanism Branches, Turning Curves and Critical Points”, *Proc. ASME 2012 Design Engineering Technical Conferences*, Paper No. DETC2012/70277, August 12-15, 2012, Chicago, IL, (2012)